Am J Transl Res 2019;11(9):6249-6261
www.ajtr.org /ISSN:1943-8141/AJTR0094010

Original Article

MicroRNAs derived from urinary exosomes act as novel biomarkers in the diagnosis of intrahepatic cholestasis of pregnancy

Pei-Yue Jiang, Xiao-Jun Zhu, Ruo-An Jiang, Yi-Na Zhang, Liu Liu, Xiao-Fu Yang

Department of Obstetrics and Gynecology, Women's Hospital, School of Medicine, Zhejiang University, Hangzhou 310006, Zhejiang Province, China

Received March 18, 2019; Accepted July 3, 2019; Epub September 15, 2019; Published September 30, 2019

Abstract: We aimed to investigate the value of cholestasis-related miRNAs in the diagnosis of intra-hepatic cholestasis of pregnancy (ICP) as well as the molecular mechanisms underlying the role of these miRNAs in the pathogenesis of ICP. In this study, electron microscopy was utilized to observe the exosomes present in the urine samples collected from both ICP patients and healthy pregnant women. Real-time PCR and area under curve (AUC) analysis were performed to predict the values of several miRNAs in the diagnosis of ICP. Bioinformatics analysis and luciferase assays were conducted to identify the target genes of miR-21, miR-29a and miR-590-3p, whose regulatory relationships were then established using real-time PCR, immunohistochemistry (IHC) assay and Western Blot. In the exosomes isolated from urine samples, several miRNAs, including miR-21, miR-29a and miR-590-3p, were differentially expressed between ICP patients and healthy pregnant women. In addition, the gene of intercellular adhesion molecule 1 (ICAM1) was identified as a shared target of miR-21, miR-29a and miR-590-3p, all of which inhibited ICAM1 expression. Therefore, up-regulated expression of miR-21, miR-29a and miR-590-3p in urinary exosomes reduced the expression of ICAM1, which in turn increased the incidence of ICP.

Keywords: Exosome, miR-21, miR-29a, miR-590-3p, urine, biomarkers, ICP

Introduction

As a syndrome specifically related to pregnancy, the incidence of intra-hepatic cholestasis of pregnancy (ICP) ranges from below 1% to above 15% in different countries [1]. ICP is featured by pruritus and abnormal liver functions. The symptoms of ICP usually become more obvious in second and third trimesters of pregnancy, and ICP patients may recover in several days after delivery. Currently, the pathogenesis of ICP has been attributed to many factors including environmental, nutritional, endocrinologic and genetic factors [1].

As a class of short non-coding RNAs (ncRNAs) of less than 25 nucleotides in length, microRNAs (miRNAs) can inhibit the expression of their target genes and hence play an essential role in the regulation of many biological processes, including cell differentiation, growth, and apoptosis [2]. The inhibitory effect of miRNAs on protein expression is generally exerted via their sequence-specific binding to the 3'un-translated regions (3'UTRs) of their target mRNAs. In the past few years, miRNAs have been shown to play critical roles in the development of human diseases [3]. Therefore, extensive studies have been carried out to search specific miRNAs that can act as biomarkers for human disorders, such as complications of pregnancy [4]. Luo et al. showed that miRNAs can be released into the circulation by exosomes [5]. In addition, some circulating miRNAs derived from trophoblasts can reflect the physiological state of pregnancy and hence can be used as diagnostic markers for pregnancy. In addition, some recent studies demonstrated the diagnostic value of circulating miRNAs in the treatment of cholestatic diseases. It was also shown that, as compared with that in urine samples collected from healthy pregnant women, the expression of hsa-miR-300 and hsa-miR-151-3p is significantly decreased in the urine samples of ICP

Table 1. Demographic and clinicopathological data of the subjects of this study

Variable	Control (N = 84)	ICP (N = 62)	*P* value
Maternal age, years	28.5 ± 5.3	29.1 ± 6.2	0.125
Gestational week	33.5 ± 2.1	33.8 ± 1.5	0.846
TBA, μmol/L	28.4 ± 3.3	27.9 ± 5.2	0.248
TBIL, μmol/L	7.6 ± 1.7	7.5 ± 2.4	0.728
DBIL, μmol/L	1.6 ± 0.4	1.7 ± 0.9	0.152
ALT, IU/L	15.6 ± 4.4	15.1 ± 3.9	0.578
AST, IU/L	17.5 ± 3.8	17.4 ± 4.1	0.792
ALP, IU/L	104.8 ±12.5	107.1 ± 12.8	0.462
GGT, IU/L	13.8 ± 3.4	14.3 ± 2.5	0.938

TBA: total bile acid; TBIL: total bilirubin; DBIL: direct bilirubin; ALT: alanine transaminase; AST: aspartate aminotransferase; ALP: alkaline phosphatase; GGT: glutamyltransferase.

patients, whereas the expression of hsa-miR-369-5p and hsa-miR-671-3p is significantly increased [6]. In addition, a negative regulatory relationship was observed between the expression of miR-369-5p and its target genes [7]. Furthermore, upon lung transplantation (LT), the expression of miR-369-5p was reduced along with the increased expression of TGF-β, a target of miR-369-5p. Interestingly, TGF-β has been reported to be implicated in the pathogenesis of ICP by reducing the synthesis of IFN-γ and TNF-α [7].

As a member of the immunoglobulin superfamily, the gene of intercellular adhesion molecule-1 (ICAM-1) encodes a 90 kDa glycoprotein expressed on the cell membrane. The ICAM-1 protein has been implicated in the adhesion of leucocytes onto the endothelium [8]. In addition, under inflammatory conditions, the expression of ICAM-1 can be detected on both the lateral side and the luminal side of endothelial cells, on which ICAM-1 has been shown to mediate the adhesion and migration of different types of leukocytes on the endothelium prior to their penetration into tissues [9]. Furthermore, the expression of ICAM-1 protein and mRNA is increased in hyperglycemia [10]. Moreover, ICAM-1 is involved in neovascularization by regulating the adhesion of EPC and by inducing angiogenesis [11]. In terms of its role in cell proliferation, ICAM-1 has been shown to promote the survival of tumor cells via the activation of AKT-mediated signaling [12]. It was also shown that the level of ICAM-1 was decreased in ICP patients, thus suggesting a possible role of ICAM-1 in the pathogenesis of ICP [13]. Past studies have shown that the expression of ICAM-1 can be regulated by multiple miRNAs including miR-590-3p [13, 14].

In this study, we investigated the miRNAs related to cholestasis and compared their expression in the exosomes isolated from ICP patients and healthy pregnant women [6, 15-20]. Furthermore, the diagnostic value of these miRNAs was evaluated using receiver operating characteristic (ROC) analysis and luciferase assays.

Materials and methods

Human subjects and sample collection

In this study, we enrolled 84 ICP patients and 62 healthy pregnant women as the experimental group and the control group, respectively. The demographic and clinicopathological data of the subjects were presented in **Table 1**. Subsequently, urine and placenta samples were collected from each subject to compare the expression of different miRNAs between the two groups. The protocols of the present study were approved by the Institutional Review Board of our hospital. In addition, signed forms of written informed consent were obtained from all participating subjects.

Isolation of exosomes from urine samples and the examination of isolated exosomes by electron microscopy

Exosomes were extracted from urine samples using a miRCURY Exosome Isolation Kit (Exiqon, Vedbaek, Denmark) following the instruction of the kit. Subsequently, the morphology and distribution of extracted exosomes were measured according to the method shown in [21]. In brief, the isolated exosomes were incubated in 50 μg/mL of Con A lectin for 1 h and then fixed in a 2.5% glutaraldehyde solution for 15 min. Subsequently, the exosomes were dehydrated by gradient ethanol and analyzed under a scanning electron microscope.

RNA isolation and real-time PCR

Total RNA of tissue and cell samples was extracted using a Trizol reagent (Invitrogen, Carlsbad, CA) according to the instruction of the kit. Subsequently, the RNA isolated from

each sample was reversely transcribed to cDNA using a PrimeScript RT Kit (Takara, Tokyo, Japan). The volume of the reverse transcription system was 10 μL. The reaction conditions of reverse transcription were as follows: reverse transcription (15 min × 3 cycles) at 37°C and 5 s of reverse transcriptase inactivation at 85°C. In the next step, real-time PCR was carried out using a SYBR TaqTM II Kit (Takara, Tokyo, Japan) on an ABI7500 real-time PCR instrument (ABI, Foster City, CA). The reaction system of real-time PCR was 50 μL, including 25 μL of SYBR Premix Ex TaqTM II (2 ×), 2 μL of upstream primer, 2 μL of downstream primer, 1 μL of ROX Reference Dye (50 ×), 4 μL of cDNA template, and 16 μL of ddH_2O. The reaction conditions of real-time PCR included 30 s of pre-denaturation at 95°C, followed by 40 cycles of denaturation for 5 s at 95°C and annealing for 30 s at 60°C. The primers of let-7c, miR-16, miR-21, miR-26a-2*, miR-29a, miR-29b, miR-30a, miR-33, miR-93*, miR-98, miR-99b, miR-106, miR-122, miR-124, miR-148a, miR-151-3p, miR-183*, miR-199b-5p, miR-200, miR-204, miR-219-3p, miR-222, miR-300, miR-302b, miR-317-3p, miR-328, miR-340-3p, miR-369-3p, miR-369-5p, miR-409-5p, miR-425, miR-450a-6p, miR-489, miR-520g, miR-524-5p, miR-526a, miR-527, miR-590-3p, miR-584, miR-623, miR-658 and miR-671-3p were designed and synthesized by Takara (Tokyo, Japan). The relative expression of above transcripts was measured using 2 μg of total RNA as the template and 2 μg of GAPDH as the internal reference. The calculation of mRNA expression was carried out using the $2^{-\Delta\Delta CT}$ method.

Cell culture and transfection

HUVEC and Hs 815.PI cells were cultured in DMEM (Thermo Fisher Scientific, Waltham, MA) supplemented with 10% fetal bovine serum. When the cells reached 90% confluence, they were detached by trypsin and then seeded into 24-well plates. On the second day, the cells were transfected by miR-21 precursors, miR-29a precursors, miR-590-3p precursors, and ICAM1 siRNA, respectively, using Lipofectamine 2000 (Invitrogen, Carlsbad, CA) according to the instructions of the manufacturer. In brief, 100 pmol of plasmid (at a final concentration of 50 nM) and 5 μL of Lipofectamine 2000 were each diluted into 250 μL of serum free Opti-MEM (Gibco, Gaitherburg, MD) and incubated for 5 min at room temperature. Subsequently, the two parts were mixed together and incubated at room temperature for 20 min, and then added onto the cells in the 24-well plate. The cells were cultured for 8 h at 37°C in 5% CO_2 before the culture medium was switched to a complete medium. At 48 h post transfection, the cells were harvested for subsequent experiments.

Vector construction, mutagenesis and luciferase assay

The potential regulatory relationship between miR-21/ICAM1, miR-590-3p/ICAM1, and miR-124/ICAM1 was predicted using an online bioinformatics tool, TagetScan (www.targetscan.org/). Subsequently, the binding sites of miR-21, miR-590-3p, and miR-124, respectively, were identified in the 3'UTR of ICAM1 mRNA. Therefore, the 3'UTR of ICAM1 mRNA containing the binding sites of miR-21, miR-590-3p, and miR-124 was amplified by PCR and cloned into a pcDNA Dual-luciferase Expression Vector (Promega, Madison, WI). At the same time, site-directed mutagenesis was carried out in the binding sites of miR-21, miR-590-3p, and miR-124, respectively, to obtain mutant ICAM1 3'UTRs corresponding to above 3 miRNAs. These mutant UTRs of ICAM1 3' were also amplified by PCR and cloned into pcDNA vector. In the next step, HUVEC and Hs 815.PI cells were co-transfected by miR-21 mimics + wild type/mutant ICAM1, miR-590-3p + wild type/mutant ICAM1, or miR-124 + wild type/mutant ICAM1, respectively, using Lipofectamine 2000. At 48 h post transfection, the luciferase activity of transfected cells was detected using a Dual luciferase detection kit (Promega, Madison, WI) on a Glomax20/20 luminometer (Promega, Madison, WI) following the instructions of the manufacturer.

Western blot analysis

An RIPA kit (Solarbio, Beijing, China) was used to extract total protein from cell and tissue samples. Subsequently, a BCA kit (Thermo Fisher Scientific, Waltham, MA) was used to quantify the concentration of isolated proteins. After being separated by polyacrylamide gel electrophoresis, the protein samples were transferred onto a NC membrane by a wet transfer method, and then blocked in 5% BSA for 1 h at room temperature. In the next step, the membrane was incubated with diluted anti-ICAM1 primary antibodies (1:1000, Abcam, Cambridge, MA) at 4°C for 12 h. After a PBS

wash, the membrane was subsequently incubated with HRP labeled secondary antibodies (1:5000, Abcam, Cambridge, MA), and then immersed into an ECL solution (Biomiga, San Diego, CA) for 30 min at room temperature. The images of the membrane were acquired using an X-ray apparatus and the protein expression of ICAM1 was calculated using β-actin as the internal reference.

Immunohistochemistry

Collected placenta tissue samples were processed into serial sections with a thickness of 4 μm. Subsequently, the sections were dried in an incubator at 60°C for 1 h. In the next step, the sections were conventionally deparaffinized using xylene and dehydrated using gradient ethanol. Thereafter, the sections were immersed in 3% H_2O_2 for 10 min to block endogenous peroxidase activity, and then washed three times with distilled water (3 min for each wash). Antigen retrieval was performed in a mixture of sodium citrate buffer solution (pH 6.0) and 0.001 M ethylene diaminetetra acetic acid (EDTA, pH 8.0) at the boiling temperature. Subsequently, the sections were cooled down to room temperature using an ice water bath. Thereafter, the sections were blocked for 20 min at room temperature in 10% normal goat serum, followed by an overnight incubation at 4°C in anti-ICAM1 primary antibodies (1:500, Abcam, Cambridge, MA). After PBS washing, the sections were incubated at 37°C for 1 h with biotin labeled secondary antibodies (1:2000, Abcam, Cambridge, MA). Subsequently, the sections were stained at 37°C for 1 h in a 1:100 solution of horseradish peroxidase labeled streptavidin, followed by 10 min of incubation with a diaminobenzidine (DAB) reagent (Abcam, Cambridge, MA) for color development. The sections treated with PBS only were used as the negative control. During the analysis, a total of 10 view fields were randomly selected from each section and their images were acquired under an inverted microscope. The percentage of ICAM1 positive cells in each view field was calculated as follows: positive expression rate of ICAM1 = number of cells positive for ICAM1 expression/total number of cells.

Statistical analysis

Statistical analyses were conducted using SPSS 21.0 (IBM, Armonk, NY). The results were expressed as mean ± standard deviations. Differences between two groups were compared by *t* test, while differences among multiple groups were compared by one-way analysis of variance. The ROC analysis was performed using NCSS software (Kaysville, UT) to compare the AUC of each exosomal miRNA in urine. A p value of < 0.05 was considered as statistically significant.

Results

Urinary exosomes could be used to study the differential expression of miRNAs between ICP patients and healthy pregnant women

According to a research on relevant literature, we chose to measure let-7c, miR-16, miR-21, miR-26a-2*, miR-29a, miR-29b, miR-30a, miR-33, miR-93*, miR-98, miR-99b, miR-106, miR-122, miR-124, miR-148a, miR-151-3p, miR-183*, miR-199b-5p, miR-200, miR-204, miR-219-3p, miR-222, miR-300, miR-302b, miR-317-3p, miR-328, miR-340-3p, miR-369-3p, miR-369-5p, miR-409-5p, miR-425, miR-450a-6p, miR-489, miR-520g, miR-524-5p, miR-526a, miR-527, miR-590-3p, miR-584, miR-623, miR-658, and miR-671-3p in this study since they were reported to be associated with cholestasis. To explore the possible association between the above miRNAs and the pathogenesis of ICP, we recruited 84 ICP patients as the experimental group and 62 healthy pregnant women as the control group, respectively. As shown in **Figure 1**, electron microscopy was utilized to observe the distribution of urinary exosomes. It was found that urinary exosomes were equally distributed between ICP and control groups, indicating that urinary exosomes were adequate samples to observe the differentiated expression of miRNAs between ICP patients and healthy pregnant women.

Several cholestasis-related miRNAs were differentially expressed between ICP and control groups

We used real-time PCR to measure the expression of miRNAs in isolated urinary exosomes. The results showed that only several miRNAs were differentially expressed between ICP and control groups. As shown in **Figure 2**, miR-21 (**Figure 2A**), miR-29a (**Figure 2B**), miR-590-3p (**Figure 2C**), miR-16 (**Figure 2D**), miR-584 (**Figure 2E**) and miR-99b (**Figure 2F**) were evidently up-regulated in the ICP group, whereas

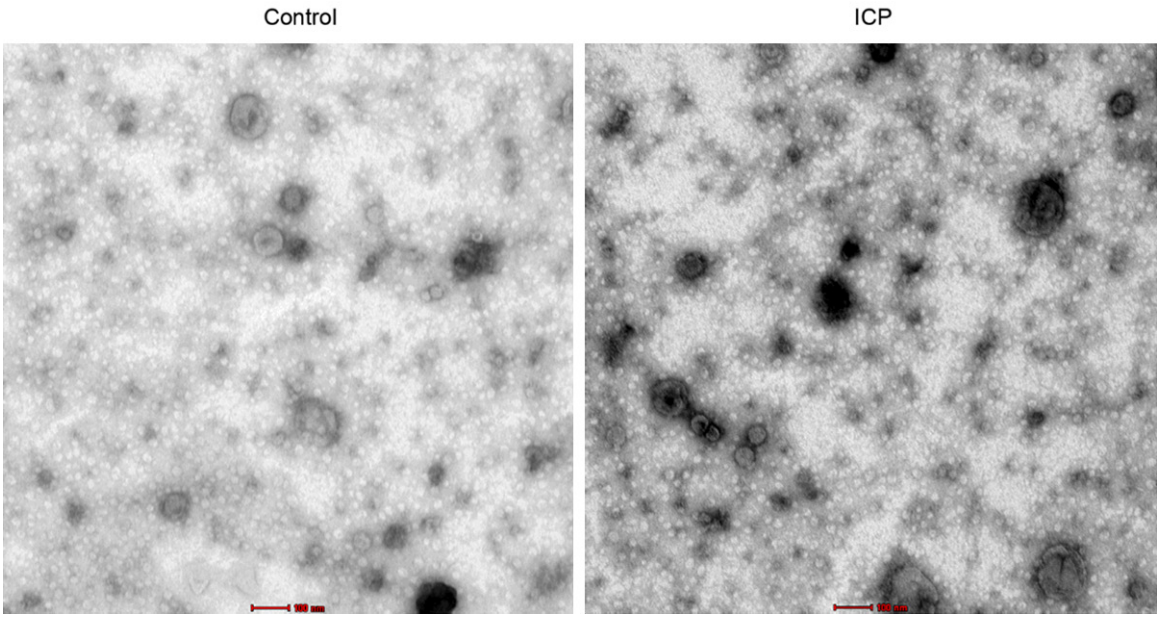

Figure 1. Distribution of urinary exosomes in samples collected from ICP patients and healthy pregnant women.

the expression of miR-151-3p (**Figure 2G**), miR-200 (**Figure 2H**), miR-122 (**Figure 2I**), miR-26a-2* (**Figure 2J**) and miR-520g (**Figure 2K**) was markedly suppressed in the ICP group.

MiR-21, miR-29a and miR-590-3p could be used as biomarkers to predict the risk of ICP

Subsequently, we conducted an ROC analysis to compare the AUC of differentially expressed miRNAs and to evaluate their diagnostic values. As demonstrated in **Figure 3**, miR-29a (**Figure 3A**), miR-590-3p (**Figure 3B**) and miR-21 (**Figure 3C**) all showed low AUC values, indicating that these miRNAs had a poor diagnostic value if they were used individually for the diagnosis of IPC. However, when these three miRNAs were analyzed in combination, the AUC of miR-29a, miR-590-3p and miR-21 (**Figure 3G**) was higher than 0.95, indicating that the group of miR-29a, miR-590-3p and miR-21 had an adequate diagnostic value in predicting the risk of ICP. Therefore, in the following sections, we searched the possible targets of miR-29a, miR-590-3p and miR-21, and studied the role of these miRNAs in the pathogenesis of IPC.

ICAM1 mRNA was a target gene of miR-21, miR-29a and miR-590-3p

By searching several common databases used for target gene prediction, specific binding sites of miR-21 (**Figure 4A**), miR-29a (**Figure 4C**) and miR-590-3p (**Figure 4E**), respectively, were identified in the 3'UTR of ICAM1 mRNA. Subsequently, miR-21 mimics, miR-29a mimics and miR-590-3p mimics, respectively, were co-transfected into cells in conjunction with wild-type/mutant 3'UTR of ICAM1 in a luciferase assay to investigate the possible regulatory relationship between ICAM1 mRNA and miR-21/miR-29a/miR-590-3p. As demonstrated in **Figure 4**, the luciferase activity of cells co-transfected with miR-21 mimics (**Figure 4B**) and wild-type ICAM1 was evidently down-regulated. Similarly, the luciferase activity of cells co-transfected with wild-type ICAM1 and miR-29a mimics (**Figure 4D**) or miR-590-3p mimics (**Figure 4F**) was also suppressed. In addition, we compared the expression of miR-21/miR-29a/miR-590-3p and ICAM1 between ICP and control groups. As demonstrated in **Figure 5**, the expression of miR-590-3p (**Figure 5A**), miR-21 (**Figure 5B**) and miR-29a (**Figure 5C**) was all elevated in the ICP group compared with that in the control group. Meanwhile, the expression of ICAM1 mRNA (**Figure 5D**) and protein (**Figure 6**) was both reduced in the ICP group compared with that in the control group. Therefore, a negative correlation could be established between ICAM1 mRNA and miR-21/miR-29a/miR-590-3p, with ICAM1 mRNA being a virtual target of these miRNAs.

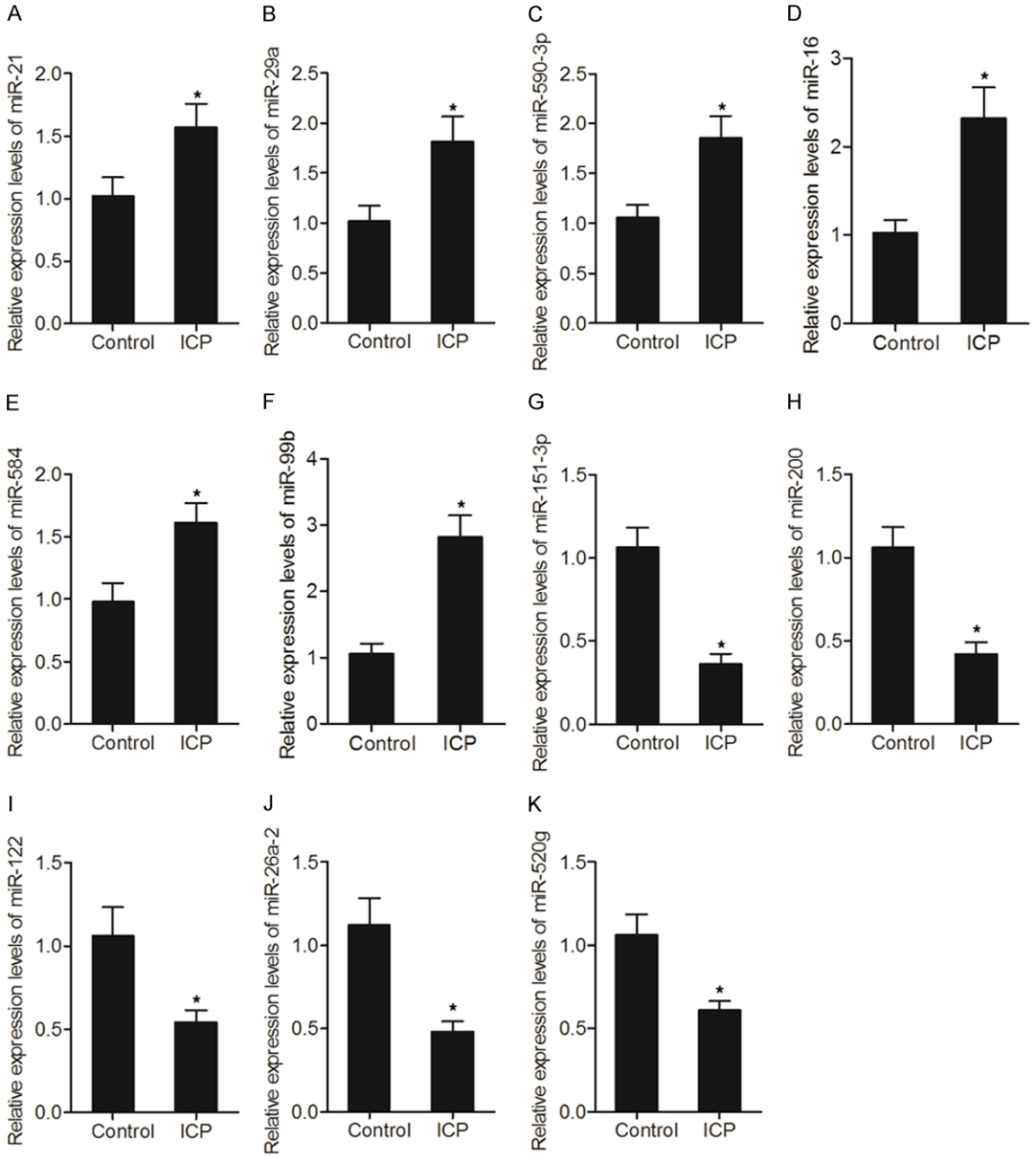

Figure 2. Differential expression of several cholestasis-related miRNAs between ICP and control groups (*P value < 0.05, vs. control group). A. Expression of miR-21 between ICP and control groups; B. Expression of miR-29a between ICP and control groups; C. Expression of miR-590-3p between ICP and control groups; D. Expression of miR-16 between ICP and control groups; E. Expression of miR-584 between ICP and control groups; F. Expression of miR-99b between ICP and control groups; G. Expression of miR-151-3p between ICP and control groups; H. Expression of miR-200 between ICP and control groups; I. Expression of miR-122 between ICP and control groups; J. Expression of miR-26a-2* between ICP and control groups; K. Expression of miR-520g between ICP and control groups.

MiR-590-3p, miR-21 and miR-29a negatively regulated the expression of ICAM1

HUVEC cells were transfected with miR-590-3p mimics, miR-21 mimics, miR-29a mimics, and ICAM1 siRNA, respectively, before the expression of ICAM1 mRNA and protein in transfected cells was measured. As shown in **Figure 7**, the mRNA and protein expression of ICAM1 was reduced in HUVEC cells transfected with miR-

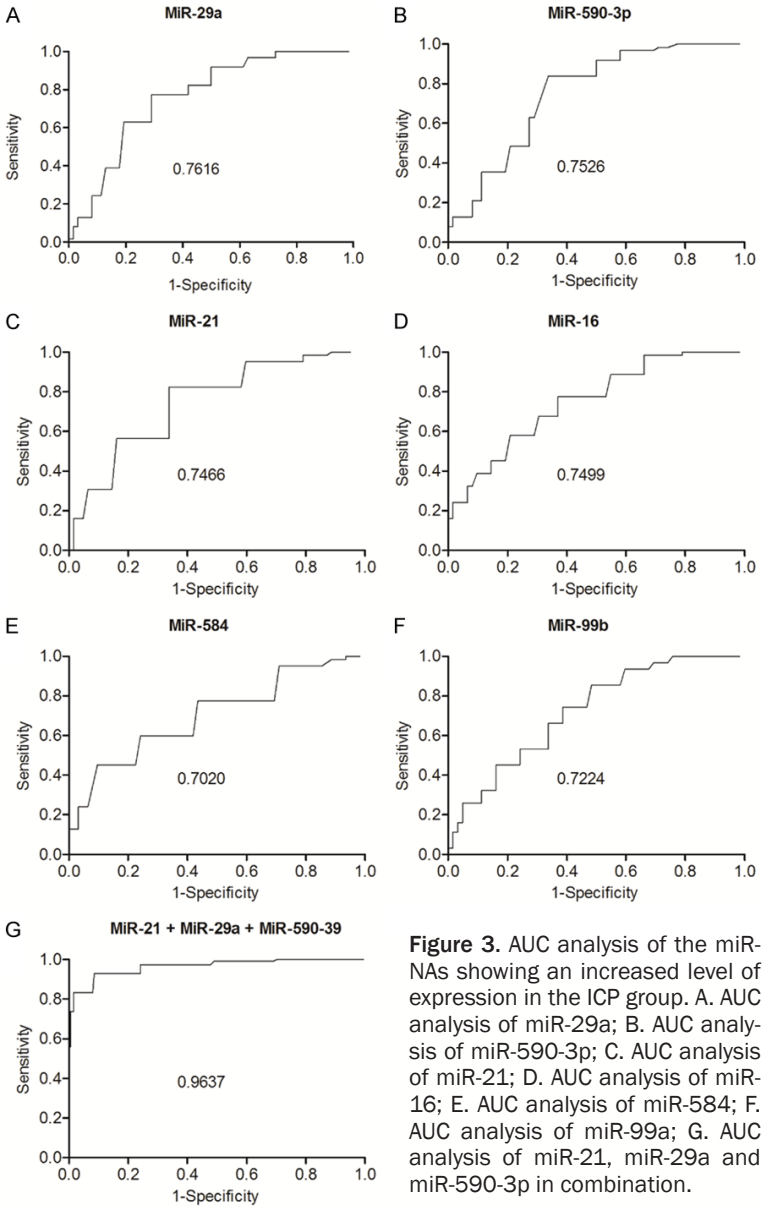

Figure 3. AUC analysis of the miRNAs showing an increased level of expression in the ICP group. A. AUC analysis of miR-29a; B. AUC analysis of miR-590-3p; C. AUC analysis of miR-21; D. AUC analysis of miR-16; E. AUC analysis of miR-584; F. AUC analysis of miR-99a; G. AUC analysis of miR-21, miR-29a and miR-590-3p in combination.

29a mimics (**Figure 7A**), miR-21 mimics (**Figure 7B**), miR-590-3p (**Figure 7C**), or ICAM1 siRNA (**Figure 7D**). Similar results were also obtained from Hs 815.PI cells (**Figure 8**), validating the inhibitory effects of miR-590-3p, miR-21 and miR-29a on ICAM1 expression. Therefore, the reduced ICAM1 expression in placenta would lead to an increased risk of ICP.

Discussion

Multiple types of extracellular vesicles are present in urine, with exosomes being the most extensively studied extracellular vesicles. As membrane vesicles of less than 100 nm in diameter, exosomes are derived from multi-vesicular bodies located in the endosomes [22]. The content of exosomes, such as miRNAs and mRNAs, can be transferred to distant receptor cells to mediate inter-cellular communication [22]. Moreover, exosomes have been used as potential non-invasive biomarkers in the diagnosis of renal diseases [23]. Unlike free miRNAs circulating in urine, the miRNAs in exosomes are highly stable since they are protected by exosomes against endogenous RNase. A previous study demonstrated that exosomes could cross the blood-brain barrier presumably through receptor-mediated transcytosis [24, 25]. Altered profiles of exosomal miRNAs have also been demonstrated in the urine samples collected from type I diabetic patients and patients of focal segmental glomerulosclerosis [26, 27]. In this study, we explored the possible association between miRNA expression and the pathogenesis of ICP by comparing the expression of cholestasis-related miRNAs between ICP patients and healthy pregnant women. The results showed that the expression of miR-21 (**Figure 2A**), miR-29a (**Figure 2B**), miR-590-3p (**Figure 2C**), miR-16 (**Figure 2D**), miR-584 (**Figure 2E**) and miR-99b (**Figure 2F**) was evidently up-regulated in the ICP group, whereas the expression of miR-151-3p (**Figure 2G**), miR-200 (**Figure 2H**), miR-122 (**Figure 2I**), miR-26a-2* (**Figure 2J**) and miR-520g (**Figure 2K**) was markedly suppressed in the ICP group. Furthermore, we performed an ROC analysis to compare the AUC of different miRNAs. The results showed that the AUC of miR-29a, miR-530-3p and miR-21 as a group was substantially higher than the AUC of each individual miRNA, indicating that these three exosomal miRNAs may be used as a group for the diagnosis of ICP.

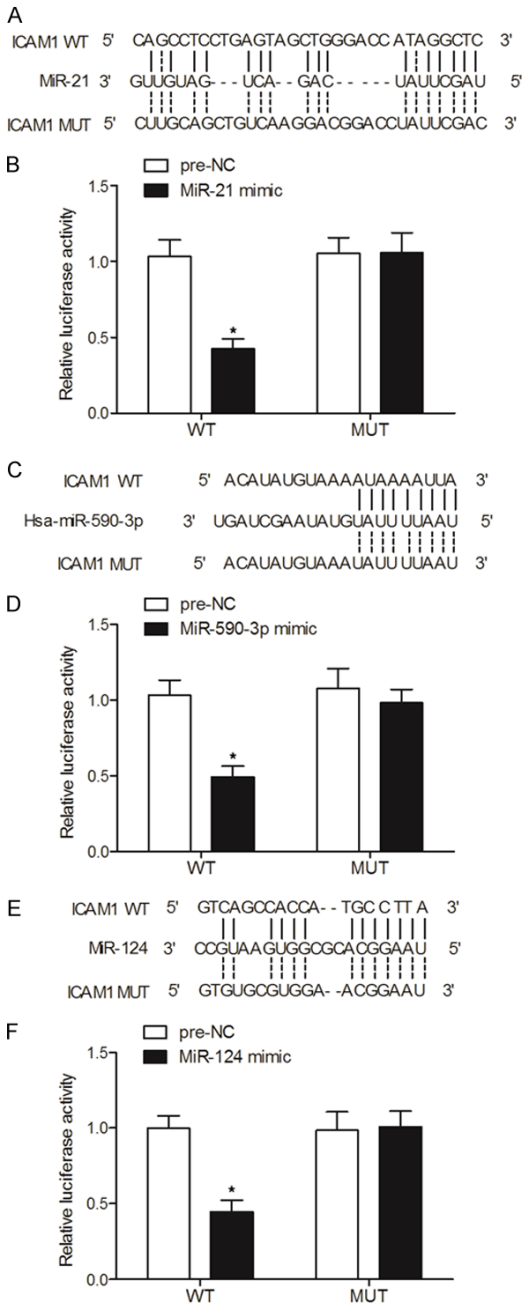

Figure 4. ICAM1 mRNA was identified as a target gene of miR-21, miR-29a and miR-590-3p via computational analysis and luciferase assays (*P value < 0.05, vs. NC group). A. Computational analysis of miR-21 and ICAM1 mRNA; B. Luciferase activity of cells co-transfected with miR-21 and wild-type/mutant ICAM1 mRNA; C. Computational analysis of miR-590-3p and ICAM1 mRNA; D. Luciferase activity of cells co-transfected with miR-590-3p and wild-type/mutant ICAM1 mRNA; E. Computational analysis of miR-29a and ICAM1 mRNA; F. Luciferase activity of cells co-transfected with miR-29a and wild-type/mutant ICAM1 mRNA.

Luo et al. showed that miRNAs can be released into blood circulation via exosomes, indicating that the miRNAs derived from trophoblasts can be used as diagnostic markers for pregnancy. In fact, as a source readily available for non-invasive diagnostic markers, urine has been used in the diagnosis of many diseases [5, 28]. In terms of the value of urine in miRNA-based diagnosis, it was shown that, as compared with their expression in urine samples collected from healthy pregnant women, the expression of hsa-miR-300 and hsa-miR-151-3p is significantly decreased in the urine samples of ICP patients, whereas the expression of hsa-miR-369-5p and hsa-miR-671-3p is significantly increased [6]. A past study has also shown that the expression of miR-29c in urinary exosomes can be utilized to predict the onset of lupus nephritis and fibrosis [29]. Chen et al. also indicated that, by inhibiting the expression of inositol polyphosphate 4-phosphatase type II, miR-590-3p induced the invasion and proliferation of prostate cancer cells [30]. Pang et al. showed that, by suppressing the expression of ZEB2 and ZEB1, miR-590-3p inhibited the epithelial-mesenchymal transition (EMT), migration, and invasion of glioblastoma cells [31]. In addition, it was demonstrated that, by binding to the 3'UTR of ICAM-1, miR-590-3p could inhibit the expression of ICAM-1 [13].

The deletion of miR-21 in a mouse model of acute pancreatitis was shown to reduce the level of necroptosis in mice [32]. Interestingly, the expression of miR-21 is up-regulated in patients suffering from cholestatic liver injury, non-alcoholic steatohepatitis, hepatocellular carcinoma and cholalgiocarcinoma [33-36]. In addition, the expression of miR-21 is elevated in many liver diseases [37]. Because miR-21 can regulate the activation of hepatic stellate and the progression of liver fibrosis in a mouse model of bile duct-ligation (BDL), miR-21 may also act as a novel target to suppress fibrosis and necroptosis-induced liver injury. Some studies have investigated the mechanisms underlying the role of miR-21 in the development of cholestasis, in which necroptosis acts as a key factor in disease progression [36, 38]. Interestingly, in patients with late stage chronic cholestasis, the concentration of deoxycholic acid (DCA) in their liver is significantly decreased compared with that in normal liver tissues [39]. Since DCA was shown to inhibit the expression of miR-21 in primary hepatocytes, the reduced DCA concentration in these patients would increase miR-21 expression and lead to an imbalance between cell apoptosis and prolifer-

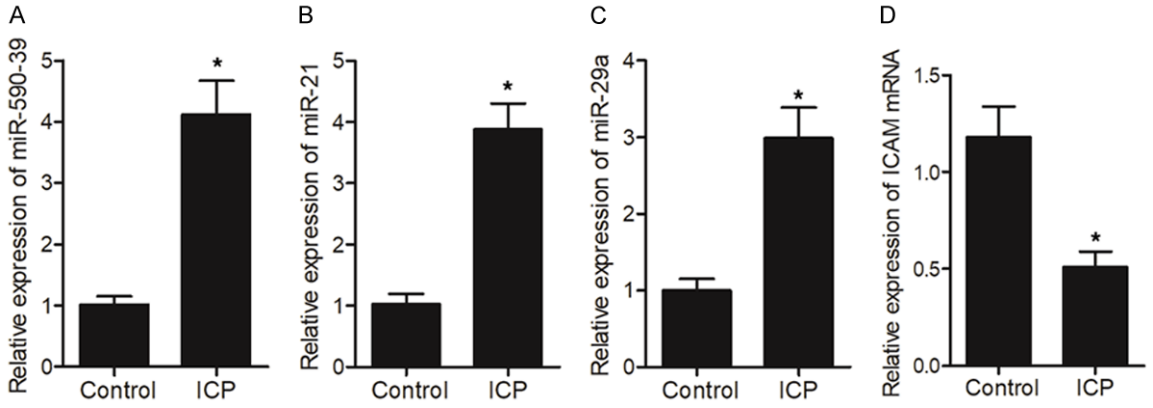

Figure 5. A negative correlation was observed between ICAM1 mRNA and miR-21/miR-29a/miR-590-3p (*P value < 0.05, vs. control group). A. Expression levels of miR-590-3p in ICP and control groups; B. Expression levels of miR-21 in ICP and control groups; C. Expression levels of miR-29a in ICP and control groups; D. Expression levels of ICAM1 mRNA in ICP and control groups.

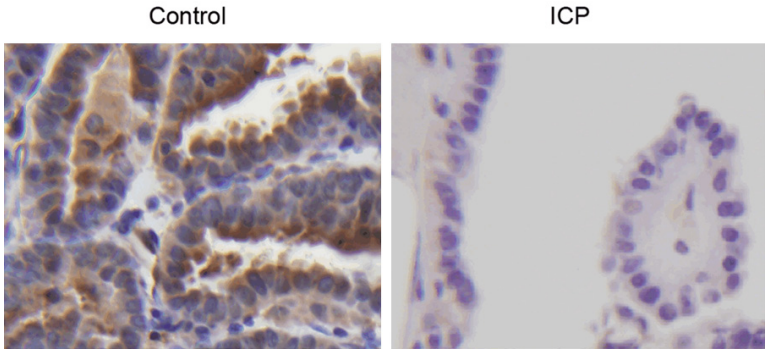

Figure 6. IHC assays on the expression of ICAM1 in ICP and control groups.

ation, thus impairing fibrogenesis and metabolic homeostasis [34, 35, 40]. It was also shown that the suppression of miR-21 expression could alleviate necroptosis and liver damages in BDL mice. Furthermore, the inhibition of miR-21 expression could potentially be used to treat cholestasis [41].

Growing evidence suggested that the reduced expression of miR-29 is implicated in the onset of liver cirrhosis and fibrosis in animal models [42]. Furthermore, activated HSCs were shown to demonstrate a high level of fibrogenic reactions because of reduced miR-29 expression [43]. Moreover, the over-expression of miR-29 was shown to reduce the accumulation of fibrotic matrix and collagen in HSCs [43]. The over-expression of miR-29a was also shown to reduce the level of hepatocellular apoptosis and suppress the activation of HSCs upon liver injury [44]. In addition, miR-29a reduces the expression of histone deacetylase 4 and TGF-1, thus alleviating BDL-induced cholestatic liver fibrosis [44]. It was also shown that the over-expression of miR-29a could significantly reduce the levels of pro-apoptotic proteins while increasing the levels of phospho-AKT proteins, thus leading to reduced apoptosis and recovery of liver injury in cholestasis [14]. Finally, the over-expression of miR-29a in a mouse model of cholestasis apparently suppressed the expression of collagen-4α1 and collagen-1α1 proteins [45].

In this study, we identified ICAM1 mRNA as a target of miR-21, miR-29a and miR-530-3p via the computational analysis. In addition, cells co-transfected with wild-type ICAM1 and miR-21/miR-29a/miR-530-3p all showed reduced luciferase activity. Therefore, a negative regulatory relationship was established between ICAM1 and miR-21/miR-29a/miR-530-3p. ICAM-1 encodes a 90 kDa glycoprotein expressed on cell membrane. The ICAM-1 protein has been implicated in the adhesion of leucocytes onto the endothelium [8]. Furthermore, the expression of ICAM-1 protein and mRNA was increased in hyperglycaemia [9]. Since angiogenesis and blood vessel regeneration are closely correlated to the growth and apoptosis of epithelial cells, the low blood vessel density

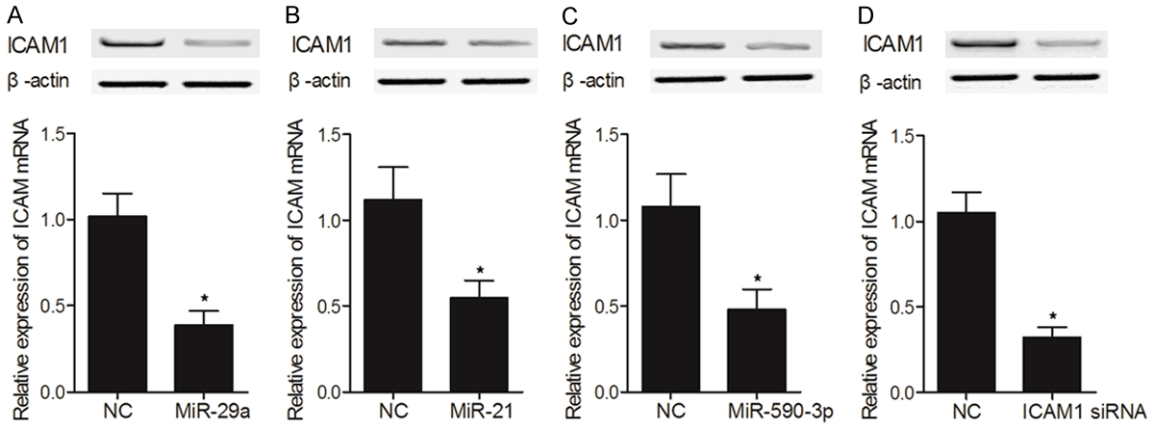

Figure 7. The negative regulatory relationship between ICAM1 and miR-21/miR-29a/miR-590-3p was validated by transfecting HUVEC cells with miR-590-3p mimics, miR-21 mimics, miR-29a mimics and ICAM1 siRNA, respectively (*P value < 0.05, vs. NC group). A. Expression of ICAM1 mRNA and protein in HUVEC cells transfected with miR-29a mimics; B. Expression of ICAM1 mRNA and protein in HUVEC cells transfected with miR-21 mimics; C. Expression of ICAM1 mRNA and protein in HUVEC cells transfected with miR-590-3p mimics; D. Expression of ICAM1 mRNA and protein in HUVEC cells transfected with ICAM1 siRNA.

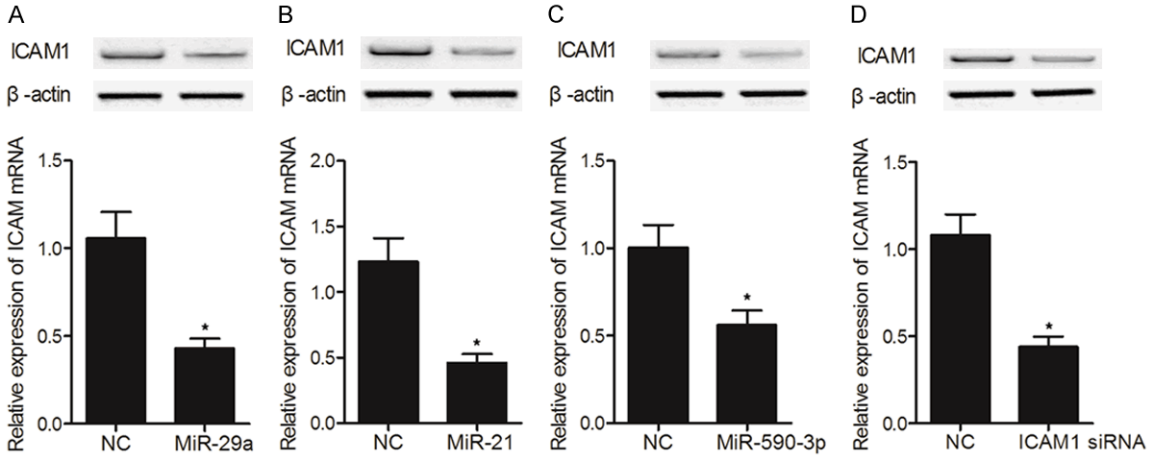

Figure 8. The negative regulatory relationship between ICAM1 and miR-21/miR-29a/miR-590-3p was validated by transfecting Hs 815.PI cells with miR-590-3p mimics, miR-21 mimics, miR-29a mimics and ICAM1 siRNA, respectively (*P value < 0.05, vs. NC group). A. Expression of ICAM1 mRNA and protein in Hs 815.PI cells transfected with miR-29a mimics; B. Expression of ICAM1 mRNA and protein in Hs 815.PI cells transfected with miR-21 mimics; C. Expression of ICAM1 mRNA and protein in Hs 815.PI cells transfected with miR-590-3p mimics; D. Expression of ICAM1 mRNA and protein in Hs 815.PI cells transfected with ICAM1 siRNA.

and smaller blood vessel size observed in ICP indicate the dysregulation of placental vascular formation and a reduced level of vascular maturation [46, 47]. Moreover, it was found that the presence of bile acid can reduce the expression of ICAM-1, a factor implicated in the pathogenesis of ICP [13]. In this study, the effects of miR-21 mimics, miR-29a mimics, miR-530-3p mimics and ICAM1 siRNA, respectively, on the mRNA and protein expression of ICAM1 were measured. When cells were treated with miR-21/miR-29a/miR-530-3p and ICAM1 siRNA, the levels of ICAM1 mRNA and protein were significantly decreased. Therefore, miR-21, miR-29a and miR-530-3p were confirmed to downregulate the expression of ICAM1.

Conclusion

Taken together, we showed that exosome-derived miR-21, miR-29a and miR-590-3p can be used as potential biomarkers for the diagno-

sis of ICP. In addition, the urinary exosomes collected from ICP patients showed significantly up-regulated expression of miR-21, miR-29a and miR-590-3p compared with the urinary exosomes collected from healthy controls. Furthermore, miR-21, miR-29a and miR-590-3p could directly target and inhibit the expression of ICAM1, an important factor implicated in the development of ICP.

Disclosure of conflict of interest

None.

Address correspondence to: Xiao-Fu Yang, Department of Obstetrics and Gynecology, Women's Hospital, School of Medicine, Zhejiang University, No. 1 Xueshi Rd, Hangzhou 310006, Zhejiang Province, China. E-mail: yangxiaofu@zju.edu.cn

References

[1] Ozkan S, Ceylan Y, Ozkan OV and Yildirim S. Review of a challenging clinical issue: intrahepatic cholestasis of pregnancy. World J Gastroenterol 2015; 21: 7134-7141.

[2] Giordano S and Columbano A. MicroRNAs: new tools for diagnosis, prognosis, and therapy in hepatocellular carcinoma? Hepatology 2013; 57: 840-847.

[3] Pal MK, Jaiswar SP, Dwivedi VN, Tripathi AK, Dwivedi A and Sankhwar P. MicroRNA: a new and promising potential biomarker for diagnosis and prognosis of ovarian cancer. Cancer Biol Med 2015; 12: 328-341.

[4] Chim SS, Shing TK, Hung EC, Leung TY, Lau TK, Chiu RW and Lo YM. Detection and characterization of placental microRNAs in maternal plasma. Clin Chem 2008; 54: 482-490.

[5] Luo SS, Ishibashi O, Ishikawa G, Ishikawa T, Katayama A, Mishima T, Takizawa T, Shigihara T, Goto T, Izumi A, Ohkuchi A, Matsubara S and Takeshita T. Human villous trophoblasts express and secrete placenta-specific microRNAs into maternal circulation via exosomes. Biol Reprod 2009; 81: 717-729.

[6] Ma L, Zhang XQ, Zhou DX, Cui Y, Deng LL, Yang T, Shao Y and Ding M. Feasibility of urinary microRNA profiling detection in intrahepatic cholestasis of pregnancy and its potential as a non-invasive biomarker. Sci Rep 2016; 6: 31535.

[7] Xu Z, Nayak D, Yang W, Baskaran G, Ramachandran S, Sarma N, Aloush A, Trulock E, Hachem R, Patterson GA and Mohanakumar T. Dysregulated microRNA expression and chronic lung allograft rejection in recipients with antibodies to donor HLA. Am J Transplant 2015; 15: 1933-1947.

[8] van de Stolpe A and van der Saag PT. Intercellular adhesion molecule-1. J Mol Med (Berl) 1996; 74: 13-33.

[9] Kado S, Wakatsuki T, Yamamoto M and Nagata N. Expression of intercellular adhesion molecule-1 induced by high glucose concentrations in human aortic endothelial cells. Life Sci 2001; 68: 727-737.

[10] Schlesinger M and Bendas G. Vascular cell adhesion molecule-1 (VCAM-1)--an increasing insight into its role in tumorigenicity and metastasis. Int J Cancer 2015; 136: 2504-2514.

[11] Silverman MD, Haas CS, Rad AM, Arbab AS and Koch AE. The role of vascular cell adhesion molecule 1/ very late activation antigen 4 in endothelial progenitor cell recruitment to rheumatoid arthritis synovium. Arthritis Rheum 2007; 56: 1817-1826.

[12] Chen Q and Massague J. Molecular pathways: VCAM-1 as a potential therapeutic target in metastasis. Clin Cancer Res 2012; 18: 5520-5525.

[13] Qin X, Ni X, Mao X, Ying H and Du Q. Cholestatic pregnancy is associated with reduced VCAM1 expression in vascular endothelial cell of placenta. Reprod Toxicol 2017; 74: 23-31.

[14] Harris TA, Yamakuchi M, Ferlito M, Mendell JT and Lowenstein CJ. MicroRNA-126 regulates endothelial expression of vascular cell adhesion molecule 1. Proc Natl Acad Sci U S A 2008; 105: 1516-1521.

[15] Nakagawa R, Muroyama R, Saeki C, Goto K, Kaise Y, Koike K, Nakano M, Matsubara Y, Takano K, Ito S, Saruta M, Kato N and Zeniya M. miR-425 regulates inflammatory cytokine production in CD4(+) T cells via N-Ras upregulation in primary biliary cholangitis. J Hepatol 2017; 66: 1223-1230.

[16] Dai BH, Geng L, Wang Y, Sui CJ, Xie F, Shen RX, Shen WF and Yang JM. microRNA-199a-5p protects hepatocytes from bile acid-induced sustained endoplasmic reticulum stress. Cell Death Dis 2013; 4: e604.

[17] Yang YL, Wang FS, Li SC, Tiao MM and Huang YH. MicroRNA-29a alleviates bile duct ligation exacerbation of hepatic fibrosis in mice through epigenetic control of methyltransferases. Int J Mol Sci 2017; 18.

[18] Shifeng H, Danni W, Pu C, Ping Y, Ju C, Liping Z. Circulating liver-specific miR-122 as a novel potential biomarker for diagnosis of cholestatic liver injury. PLoS One 2013; 8: e73133.

[19] Xiao Y, Wang J, Yan W, Zhou Y, Chen Y, Zhou K, Wen J, Wang Y and Cai W. Dysregulated miR-124 and miR-200 expression contribute to cholangiocyte proliferation in the cholestatic liver by targeting IL-6/STAT3 signalling. J Hepatol 2015; 62: 889-896.

[20] Rao ZZ, Zhang XW, Ding YL and Yang MY. miR-148a-mediated estrogen-induced chole-

stasis in intrahepatic cholestasis of pregnancy: role of PXR/MRP3. PLoS One 2017; 12: e0178702.
[21] Kosanovic M and Jankovic M. Isolation of urinary extracellular vesicles from tamm-horsfall protein-depleted urine and their application in the development of a lectin-exosome-binding assay. Biotechniques 2014; 57: 143-149.
[22] van Balkom BW, Pisitkun T, Verhaar MC and Knepper MA. Exosomes and the kidney: prospects for diagnosis and therapy of renal diseases. Kidney Int 2011; 80: 1138-1145.
[23] Miranda KC, Bond DT, McKee M, Skog J, Paunescu TG, Da Silva N, Brown D and Russo LM. Nucleic acids within urinary exosomes/microvesicles are potential biomarkers for renal disease. Kidney Int 2010; 78: 191-199.
[24] Alvarez-Erviti L, Seow Y, Yin H, Betts C, Lakhal S and Wood MJ. Delivery of siRNA to the mouse brain by systemic injection of targeted exosomes. Nat Biotechnol 2011; 29: 341-345.
[25] S ELA, Mager I, Breakefield XO and Wood MJ. Extracellular vesicles: biology and emerging therapeutic opportunities. Nat Rev Drug Discov 2013; 12: 347-357.
[26] Ramezani A, Devaney JM, Cohen S, Wing MR, Scott R, Knoblach S, Singhal R, Howard L, Kopp JB and Raj DS. Circulating and urinary microRNA profile in focal segmental glomerulosclerosis: a pilot study. Eur J Clin Invest 2015; 45: 394-404.
[27] Barutta F, Tricarico M, Corbelli A, Annaratone L, Pinach S, Grimaldi S, Bruno G, Cimino D, Taverna D, Deregibus MC, Rastaldi MP, Perin PC and Gruden G. Urinary exosomal microRNAs in incipient diabetic nephropathy. PLoS One 2013; 8: e73798.
[28] Dubin PH, Yuan H, Devine RK, Hynan LS, Jain MK and Lee WM. Micro-RNA-122 levels in acute liver failure and chronic hepatitis C. J Med Virol 2014; 86: 1507-1514.
[29] Sole C, Cortes-Hernandez J, Felip ML, Vidal M and Ordi-Ros J. miR-29c in urinary exosomes as predictor of early renal fibrosis in lupus nephritis. Nephrol Dial Transplant 2015; 30: 1488-1496.
[30] Tetzlaff MT, Curry JL, Yin V, Pattanaprichakul P, Manonukul J, Uiprasertkul M, Manyam GC, Wani KM, Aldape K, Zhang L, Prieto VG and Esmaeli B. Distinct pathways in the pathogenesis of sebaceous carcinomas implicated by differentially expressed microRNAs. JAMA Ophthalmol 2015; 133: 1109-1116.
[31] Mo M, Peng F, Wang L, Peng L, Lan G and Yu S. Roles of mitochondrial transcription factor A and microRNA-590-3p in the development of bladder cancer. Oncol Lett 2013; 6: 617-623.
[32] Ma X, Conklin DJ, Li F, Dai Z, Hua X, Li Y, Xu-Monette ZY, Young KH, Xiong W, Wysoczynski M, Sithu SD, Srivastava S and Bhatnagar A. The oncogenic microRNA miR-21 promotes regulated necrosis in mice. Nat Commun 2015; 6: 7151.
[33] Selaru FM, Olaru AV, Kan T, David S, Cheng Y, Mori Y, Yang J, Paun B, Jin Z, Agarwal R, Hamilton JP, Abraham J, Georgiades C, Alvarez H, Vivekanandan P, Yu W, Maitra A, Torbenson M, Thuluvath PJ, Gores GJ, LaRusso NF, Hruban R and Meltzer SJ. MicroRNA-21 is overexpressed in human cholangiocarcinoma and regulates programmed cell death 4 and tissue inhibitor of metalloproteinase 3. Hepatology 2009; 49: 1595-1601.
[34] Meng F, Henson R, Wehbe-Janek H, Ghoshal K, Jacob ST and Patel T. MicroRNA-21 regulates expression of the PTEN tumor suppressor gene in human hepatocellular cancer. Gastroenterology 2007; 133: 647-658.
[35] Dattaroy D, Pourhoseini S, Das S, Alhasson F, Seth RK, Nagarkatti M, Michelotti GA, Diehl AM and Chatterjee S. Micro-RNA 21 inhibition of SMAD7 enhances fibrogenesis via leptin-mediated NADPH oxidase in experimental and human nonalcoholic steatohepatitis. Am J Physiol Gastrointest Liver Physiol 2015; 308: G298-312.
[36] Kennedy LL, Meng F, Venter JK, Zhou T, Karstens WA, Hargrove LA, Wu N, Kyritsi K, Greene J, Invernizzi P, Bernuzzi F, Glaser SS, Francis HL and Alpini G. Knockout of microRNA-21 reduces biliary hyperplasia and liver fibrosis in cholestatic bile duct ligated mice. Lab Invest 2016; 96: 1256-1267.
[37] Tan Y, Pan T, Ye Y, Ge G, Chen L, Wen D and Zou S. Serum microRNAs as potential biomarkers of primary biliary cirrhosis. PLoS One 2014; 9: e111424.
[38] Afonso MB, Rodrigues PM, Simao AL, Ofengeim D, Carvalho T, Amaral JD, Gaspar MM, Cortez-Pinto H, Castro RE, Yuan J and Rodrigues CM. Activation of necroptosis in human and experimental cholestasis. Cell Death Dis 2016; 7: e2390.
[39] Fischer S, Beuers U, Spengler U, Zwiebel FM and Koebe HG. Hepatic levels of bile acids in end-stage chronic cholestatic liver disease. Clin Chim Acta 1996; 251: 173-186.
[40] Rodrigues PM, Afonso MB, Simao AL, Borralho PM, Rodrigues CM and Castro RE. Corrigendum: inhibition of NF-kappaB by deoxycholic acid induces miR-21/PDCD4-dependent hepatocellular apoptosis. Sci Rep 2016; 6: 27828.
[41] Afonso MB, Rodrigues PM, Simao AL, Gaspar MM, Carvalho T, Borralho P, Banales JM, Castro RE and Rodrigues CMP. miRNA-21 ablation protects against liver injury and necroptosis in cholestasis. Cell Death Differ 2018; 25: 857-872.

[42] Huang YH, Chuang JH, Yang YL, Huang CC, Wu CL and Chen CL. Cholestasis downregulate hepcidin expression through inhibiting IL-6-induced phosphorylation of signal transducer and activator of transcription 3 signaling. Lab Invest 2009; 89: 1128-1139.

[43] Roderburg C, Urban GW, Bettermann K, Vucur M, Zimmermann H, Schmidt S, Janssen J, Koppe C, Knolle P, Castoldi M, Tacke F, Trautwein C and Luedde T. Micro-RNA profiling reveals a role for miR-29 in human and murine liver fibrosis. Hepatology 2011; 53: 209-218.

[44] Li SC, Wang FS, Yang YL, Tiao MM, Chuang JH and Huang YH. Microarray study of pathway analysis expression profile associated with microRNA-29a with regard to murine cholestatic liver injuries. Int J Mol Sci 2016; 17: 324.

[45] Tiao MM, Wang FS, Huang LT, Chuang JH, Kuo HC, Yang YL and Huang YH. MicroRNA-29a protects against acute liver injury in a mouse model of obstructive jaundice via inhibition of the extrinsic apoptosis pathway. Apoptosis 2014; 19: 30-41.

[46] Yin Y, Zhu QY, Ren SJ and Wang DM. Increased lectin-like oxidized LDL receptor-1 expression in the placentas of women with intrahepatic cholestasis during pregnancy. Clin Exp Obstet Gynecol 2012; 39: 149-152.

[47] Du Q, Pan Y, Zhang Y, Zhang H, Zheng Y, Lu L, Wang J, Duan T and Chen J. Placental gene-expression profiles of intrahepatic cholestasis of pregnancy reveal involvement of multiple molecular pathways in blood vessel formation and inflammation. BMC Med Genomics 2014; 7: 42.